



<http://dx.doi.org/10.12702/iii.inovagri.2015-a010>

ENERGY BALANCE WITH LANDSAT 8 SATELLITE IMAGES IN IRRIGATED AREAS OF JUAZEIRO MUNICIPALITY

Antônio Heriberto de Castro Teixeira¹, Janice Freitas Leivas¹, Ricardo Guimarães Andrade¹,
and Fernando Braz Tangerino Hernandez²

ABSTRACT: Landsat 8 satellite images were used with the SAFER (Simple Algorithm For Evapotranspiration Retrieving) algorithm for the energy balance quantification in irrigated crops inside the Juazeiro municipality, Northeast Brazil, involving different thermohydrological conditions of the years 2013 and 2014. Two images represented the wet conditions soon after the rainy period (May-June), while the other ones were inside the driest period (September-October). The average values for the global solar radiation (R_G) ranged from 19.6 ± 0.5 to 26.2 ± 0.2 MJ m⁻² day⁻¹ while for the net radiation (R_n) this range was from 8.2 ± 0.2 to 11.9 ± 0.3 MJ m⁻² day⁻¹. The mean latent λE and sensible H heat fluxes were, respectively, from 7.5 ± 3.3 to 10.5 ± 2.3 and -2.1 ± 2.3 to 4.0 ± 3.3 MJ m⁻² day⁻¹. Soil heat fluxes (G) under all irrigation conditions were around 0.4 ± 0.1 MJ m⁻² dia⁻¹. Shortly after the rainfall season, the fractions of R_n used as λE were 112 and 119% for respectively 2013 and 2014. The corresponding values for the driest period were 0.63 and 0.98. The negative H and higher λE than R_n which happened in large areas soon after the rainy period indicated horizontal heat advection from the vicinities of the irrigated crops.

Keywords: latent heat flux, sensible heat flux, soil heat flux.

BALANÇO DE ENERGIA COM IMAGENS DO SATÉLITE LANDSAT 8 EM ÁREAS IRRIGADAS DO MUNICÍPIO DE JUAZEIRO

RESUMO: Imagens do satélite Landsat 8 foram usadas com o algoritmo SAFER (*Simple Algorithm For Evapotranspiration Retrieving*) para a quantificação do balanço de energia nas culturas irrigadas do município de Juazeiro, Nordeste do Brasil, abrangendo diferentes

¹Researchers, Embrapa Satellite Monitoring, CEP 13070-15, Campinas-SP. Phone: 55 (19) 32116200, E-mails: heriberto.teixeira@embrapa.br; janice.leivas@embrapa.br; ricardo.andrade@embrapa.br

² Professor, São Paulo State University, Ilha Solteira-SP. fbhtang@agr.feis.unesp.br

condições termo hidrológicas nos anos de 2013 e 2014. Duas das imagens representaram as condições úmidas logo após o período chuvoso (maio a junho) enquanto as outras foram dentro do período de condições climáticas mais secas (setembro a outubro). Os valores médios dos pixels para radiação solar global (R_G) variaram de $19,6 \pm 0,5$ a $26,2 \pm 0,2$ MJ m⁻² dia⁻¹ enquanto que para o saldo de radiação (R_n) esta faixa foi de $8,2 \pm 0,2$ a $11,9 \pm 0,3$ MJ m⁻² dia⁻¹. Para os fluxos de calor latente (λE) e calor sensível (H) estes estiveram respectivamente nas faixas de $7,5 \pm 3,3$ a $10,5 \pm 2,3$ e $-2,1 \pm 2,3$ a $4,0 \pm 3,3$ MJ m⁻² dia⁻¹. O fluxo de calor no solo (G) para todas as condições irrigadas esteve em torno de $0,4 \pm 0,1$ MJ m⁻² dia⁻¹. Logo após o período chuvoso as frações de R_n usadas com λE foram de 112 e 119%, para respectivamente, 2013 e 2014. Os valores correspondentes para o período mais seco foram de 0,63 e 0,98. H negativo e λE maior que R_n em largas áreas ocorreram logo após o período chuvoso indicando aporte adicional de energia por advecção das áreas vizinhas às culturas irrigadas.

Palavras-chave: fluxo de calor latente, fluxo de calor sensível, fluxo de calor no solo.

INTRODUCTION

The municipality of Juazeiro, Bahia State, Brazil, became an important agricultural growing region, as a result of the modern irrigation technologies at the Low-Middle São Francisco river basin. Under these conditions of land use changes, the use of remote sensing by satellite images for quantification the energy exchanges on large scale is highly relevant what has been done in distinct climate regions (Pôças et al. 2013, Teixeira et al., 2014).

Although the worldwide known SEBAL algorithm had been calibrated and validated with field radiation and energy balance measurements, presenting a good performance in the Brazilian semi-arid region (Teixeira et al. 2009a,b), the major difficult for its applicability for the whole year is the assumption of zero λE for dry pixels. During the rainy season, the mixed ecosystems of irrigated crops and natural vegetation are homogenously wet with the whole region presenting high evapotranspiration rates.

Two algorithms were developed and validated under the Brazilian semi-arid conditions. The SAFER (Simple Algorithm For Evapotranspiration Retrieving) to acquire λE and the SUREAL (Surface Resistance Algorithm) for estimation of the surface resistance to the water fluxes (r_s). This last model allows the classification of irrigated crops in mixed agro-ecosystems (Teixeira et al., 2004)

The objective of the current research was to apply these models together with Landsat 8 images and a net of agrometeorological stations for quantification of the large-scale energy

balance components in a selected area with mixed irrigated crops in the Juazeiro municipality, Bahia state, Brazilian Northeast, under different thermohydrological conditions in the years 2013 and 2014. The results can subsidize criteria for political decisions when aiming a rational water resources management in the actual situation of fast replacement of natural vegetation species by irrigated crops. The success of the modelling here may give more confidence for the test and validations in other environments, which probably will need only calibrations of the original equations.

MATERIAL AND METHODS

Fig. 1 shows the locations of the Juazeiro municipality in the Brazilian Northeast region together the study area and the agrometeorological stations (AS).

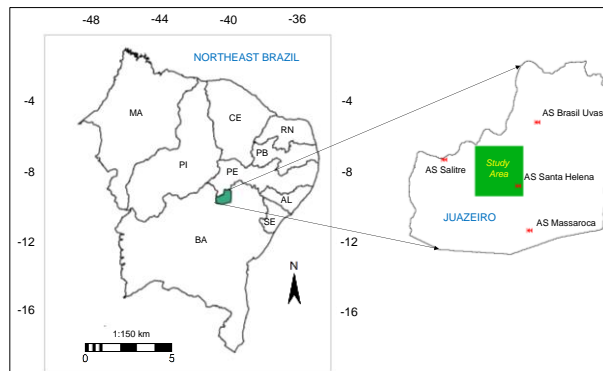


Figure 1. Location of the Juazeiro municipality, the study area and the agrometeorological stations (AS) in the Northeast region of Brazil.

Data from four automatic agrometeorological stations (AS) were used together with 4 Landsat 8 images acquired under different days of the year (DOY), being two for 2013 (DOY 150 and 278) and two for 2014 (DOY 153 and 265). Grids of global solar radiation (R_G), air temperature (T_a) and reference evapotranspiration (ET_0) were used together with remotely sensed retrieved parameters during the estimation of the large-scale energy balance components.

The bands 1 to 7 of the Landsat 8 were used for the surface albedo (α_0) calculation, while for the surface temperature (T_0), the bands 10 and 11 were used, following the methodology described in Teixeira et al. (2009a, 2014) for the Landsat 5 and 7 but considering the wavelengths and the conversion constants for the Landsat 8.

Daily R_n was calculated by using the Slob equation:

$$R_n = (1 - \alpha_0)R_G - a_L \tau_{sw} \quad (1)$$

where a_L is the regression coefficient (Teixeira et al., 2014).

The SAFER (Simple Algorithm For Evapotranspiration Retrieving) algorithm was used for modeling the instantaneous values of the ratio ET/ET_0 , which was multiplied by the grids of ET_0 for estimating the daily ET large-scale values and then transformed into energy units to give λE :

$$\frac{ET}{ET_0} = \exp \left[a_s + b_s \left(\frac{T_0}{\alpha_0 NDVI} \right) \right] \quad (2)$$

where a_s and b_s are the regressions coefficients, being 1.8 and -0.008, respectively, for the Brazilian Northeast conditions (Teixeira et al., 2014).

For the daily G values, the equation derived by Teixeira et al. (2014) was used:

$$\frac{G}{R_n} = a_G \exp(b_G \alpha_0) \quad (3)$$

where a_G and b_G are regression coefficients found to be 3.98 and -25.47, respectively for the Brazilian Northeast conditions.

The sensible heat flux (H) was estimated as residue in the energy balance equation:

$$H = R_n - \lambda E - G \quad (4)$$

The evaporative fraction (E_f) was included to take into account the soil moisture:

$$E_f = \frac{\lambda E}{R_n - G} \quad (5)$$

For classification of the vegetated surface as irrigated crops the SUREAL (Surface Resistance Algorithm) model was applied:

$$r_s = \exp \left[a_r \left(\frac{T_0}{\alpha_0} \right) (1 - NDVI) + b_r \right] \quad (6)$$

where a_r and b_r are regression coefficients, considered respectively 0.04 e 2.72 for the Brazilian Northeast condition (Teixeira et al., 2014). Pixels with r_s values bellow 800 s m^{-1} and NDVI above or equal to 0.4 were considered as irrigated crops.

RESULTS AND DISCUSSION

As the weather-driving forces for the energy partition are R_G , precipitation (P), and the atmospheric demand, represented by the reference evapotranspiration (ET_0), the trend of these weather parameters on a daily scale, during the years comprising the acquisitions of the satellite images (2013 and 2014) were first analysed. Fig. 2 shows these parameters in terms

of Day of the Year (DOY), with data from the AS Massaroca (see Fig. 1). This station was chosen because there were no data gaps.

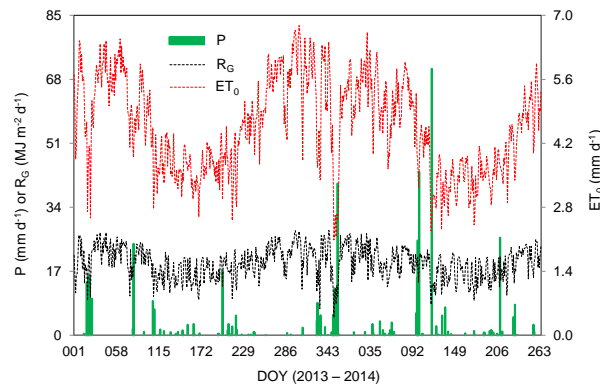


Figure 2. Daily values precipitation (P), global solar radiation (R_G) and reference evapotranspiration (ET_0) during the years 2013 and 2014 from January 2013 to September 2014, in the agrometeorological station (AS) of Massaroca, Juazeiro-BA, Northeast Brazil.

Taking into account the natural water input in the water balance, P was the most variable weather parameter. Keeping in mind that accumulated precipitations (P_{ac}) before the satellite images dates will affect the energy balance, the periods considered were from the January 01 of 2013 to September 22 of 2014 (DOY 265). The P_{ac} values were 107 and 201 mm, for DOY 150 and 153, of 2013 and 2014, respectively, while ET_{0ac} values were 721 and 705 mm. These results produced P_{ac}/ET_{0ac} values of 0.15 and 0.28, showing that the soil moisture represented by the satellite image DOY 150/2013 was lower than that for DOY 153/2014. R_G levels presented low amplitudes as the study area is close to the equator, with values without significant differences between these days, averaging $20 \text{ MJ m}^{-2} \text{ d}^{-1}$. During the driest periods of the year, represented by the images of DOY 278/2013 and 265/2014, P_{ac} levels were respectively 148 and 265 mm. In this case, with ET_{0ac} of 1265 and 1154 mm, the P_{ac}/ET_{0ac} values were 0.12 and 0.22. Although during this driest period of the year R_G increases continuously, there were no big differences between the years, with R_G around $25 \text{ MJ m}^{-2} \text{ d}^{-1}$.

Fig. 3 presents the spatial distribution of the model input parameters obtained from Landsat 8 satellite measurements, involving different agro-ecosystems, related to vegetation and soil moisture conditions, and then to the large-scale energy balance, for different periods of 2013 and 2014, in the study area of Juazeiro (BA) municipality, Northeast of Brazil.

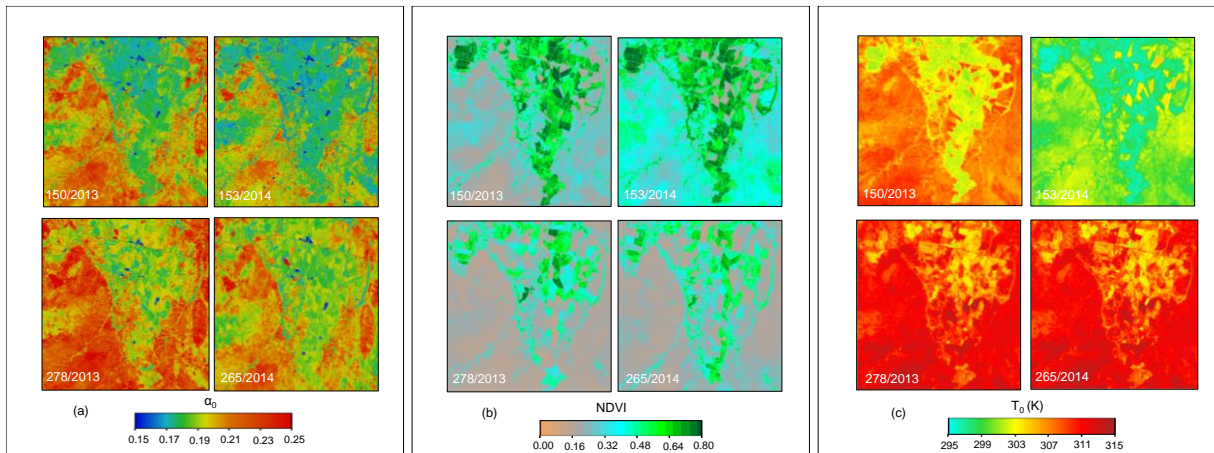


Figure 3. Spatial distribution of the model input remote sensing parameters, involving different agro-ecosystems, in study area of the Juazeiro municipality, Bahia (BA) state, Northeast of Brazil: (a) surface albedo (α_0); (b) NDVI; and (c) surface temperature (T_0).

Considering all agro-ecosystems, the α_0 average values ranged from 0.19 to 0.21, while this range for irrigated conditions was between 0.17 and 0.19. The lowest values were for DOY/Year 153/2014, while the maximums happened on DOY/Year 278/2013, when the levels of R_G were the highest, however they are also related to lower soil moisture conditions (van Dijk et al., 2004, Li et al., 2006).

The differentiation among the NDVI values along the years and agro-ecosystems are more evident than for α_0 (Figure 3b), being the largest distinctions between irrigated crops and other natural vegetation under the driest conditions from September to October (DOY/Year 278/2013 and 265/2014). The NDVI average values involving all ecosystems ranged from 0.26 (DOY/Year 278/2013) to 0.45 (DOY/Year/2014), while for irrigated crops they were between 0.57 and 0.68. In this case high both R_G and soil moisture levels promoted larger NDVI values.

The lowest T_0 values are for irrigated crops when comparing with natural vegetation (Figure 3c). In general, the periods with the highest T_0 values coincide with those with the largest R_G levels (and the lowest ones occurring after the rainy season. The average range for all agro-ecosystems was from 299.8 K (DOY/Year 153/2014) to 310.2 K (DOY/Year 278/2013), while for irrigated conditions the corresponding values were 297.3 K and 305.9 K.

Fig. 4 shows the spatial distribution of the net radiation (R_n) daily values in the study area of the Juazeiro municipality, Bahia (BA) state, Northeast of Brazil, for different periods of 2013 and 2014, in the study area of Juazeiro (BA) municipality, Northeast of Brazil.

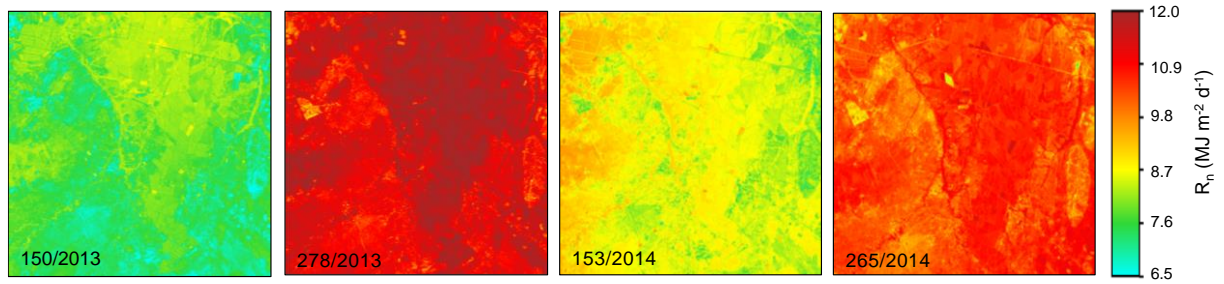


Figure 4. Spatial distribution of the large-scale daily values of net radiation (R_n) in the study area of the Juazeiro municipality, Bahia (BA) state, Northeast of Brazil, for each day of the year (DOY/Year), involving different thermo-hydrological conditions.

In general, there was no clear distinction between the R_n values between irrigated crops and natural vegetation. Also there is no big spatial variation, being evidenced a strong dependence of R_n values in R_G levels (see Fig. 2 and 4), independently of the type of vegetation, with the average values for the whole area ranging from $7.7 \text{ MJ m}^{-2} \text{ d}^{-1}$ (DOY/Year 150/2013) to $11.4 \text{ MJ m}^{-2} \text{ d}^{-1}$ (DOY/Year 278/2013). Then, the differences between these ecosystems would only arise when considering the energy partition between λE , H and G according to the thermohydrological conditions.

Fig. 5 presents the spatial distribution of the energy balance components in the selected study area of the Juazeiro municipality, Bahia (PE) state, Northeast of Brazil, for each DOY/Year, involving different thermo-hydrological conditions.

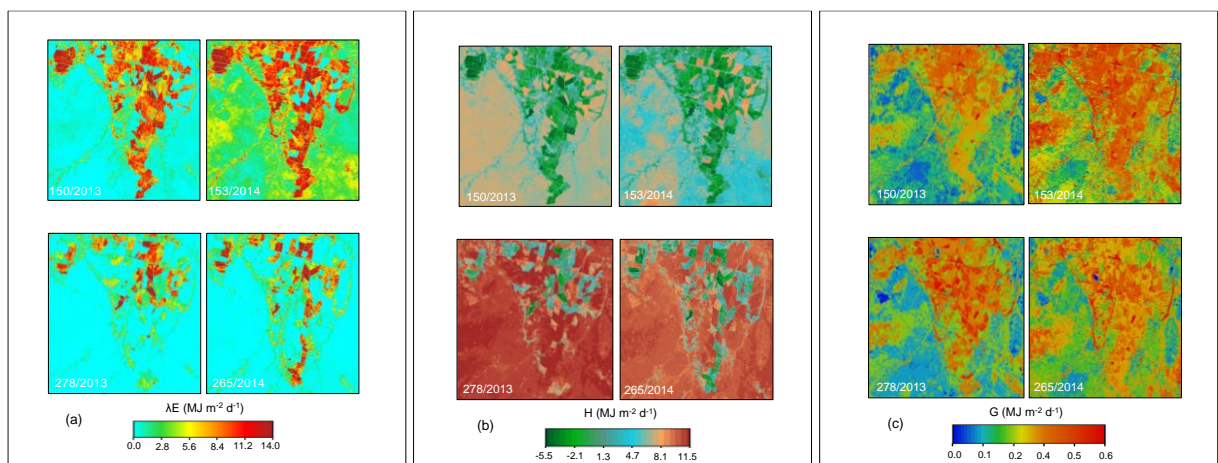


Figure 5. Spatial distribution of the large-scale daily values of the energy fluxes in different ecosystems of the study area in the Juazeiro municipality, Bahia (BA) state, Northeast of Brazil, for each day of the year (DOY/Year), involving different thermo-hydrological conditions. (a) latent heat flux – λE ; (b) sensible heat flux – H ; and (c) soil heat flux – G .

Clearly one can distinguish irrigated areas from natural vegetation by the highest λE pixel values in the first ecosystem (Fig. 5a). In some places one can see λE higher than R_n ,

mainly representing well irrigated plots. Considering all study area, the largest λE values were for DOY/Year 153/2014, averaging $4.5 \text{ MJ m}^{-2} \text{ d}^{-1}$, because the joint effect of the remaining soil moisture from rains in the root zones of natural vegetation together the irrigation in crops. The lowest ones were for DOY/Year 278/2013, with mean value of $1.3 \text{ MJ m}^{-2} \text{ d}^{-1}$.

From Fig. 5b, also, easily one can distinguish the irrigated crops from the natural vegetation, but in this case by the lower H values for the first type of vegetation. H is even negative in some occasions under irrigation conditions, due heat advection from the hotter areas at the vicinities of the crops. This fact is more noted in the middle of the year (DOY/Year 150/2013 and 153/2014), winter solstice time in the South hemisphere. Considering all the study area, in October (DOY/Year 278/2013), H presented its highest value, averaging $9.9 \text{ MJ m}^{-2} \text{ day}^{-1}$.

Another energy balance parameter that also presented differences among the semi-arid ecosystems was G (Figure 5c). At the daily scale, cropped area presented higher value than natural vegetation, what can be explained by lower negative fluxes at night. However, considering all agro-ecosystems, G pixel values were low, around $0.3 \text{ MJ m}^{-2} \text{ d}^{-1}$, and could be neglected at daily scale (Teixeira et al., 2014).

The mean pixel values of the energy balance components for the mixed irrigated crops are showed for different thermo-hydrological conditions in the selected area of the Juazeiro (BA) municipality, Northeast of Brazil (Table 1). The average R_n/R_G value ranged from 0.40 to 0.50. Field measurements retrieved R_n being 46% of R_G for wine grape, 55% for table grape, 51% for mango orchard, and 53% for “Caatinga” in the Brazilian semiarid conditions (Teixeira et al., 2008). Considering the spatial variations in R_G and R_n , represented by the standard deviations, the current results are also in agreement with other studies (Hughes et al., 2001; Yunusa et al., 2004), which give confidence to the remote sensing methods.

The highest fractions of the daily available energy (R_n) used as λE were soon after the rainy periods, when they were 112 and 119% for the DOY/Year 150/2013 and 153/2014, respectively. λE larger than R_n means horizontal heat advection from the warmer natural vegetation to the wetter irrigated crops. The H/R_n values were higher in the driest period represented by the image for the DOY/Year 278/2013, when it was 34%. For the other images H was negative, mainly in the DOY/Year 153/2014. G represented only 3 to 5% of R_n , with the lowest fractions during the driest conditions of the years. As E_f is a soil moisture indicator, one can see from Table 1 that the wettest conditions were for the DOY/Year 153/2014 and the driest ones were represented by the image of DOY/Year 278/2013.

CONCLUSIONS

Remote sensing parameters from Landsat 8 satellite images and data from a net of agrometeorological stations were coupled. This combination allowed the large-scale energy balance assessments in a mixture of irrigated crops in the Juazeiro municipality, Northeast Brazil, under different thermohydrological conditions. It was demonstrated that these analyzes can be done from instantaneous measurements of the visible, near infrared and thermal radiations of the Landsat 8 bands. This was possible by modeling the ratio of the actual to reference evapotranspiration at the satellite overpass time, and with the availability of daily weather data, providing spatial and temporal information on the energy fluxes as well plant responses to dynamic weather and irrigation conditions. Net radiation was mostly influenced by the solar radiation conditions than the characteristics of different kinds of vegetation. The mean fractions of latent, sensible and soil heat fluxes to net radiation were respectively 98, -2% and 4% for irrigated crops. In most occasions heat fluxes coming from the natural dryer areas near agricultural crops was observed.

ACKNOWLEDGMENTS

National Council for Scientific and Technological Development (CNPq) is acknowledged for the financial support to the projects on Water Productivity in Brazil.

REFERENCES

- HUGHES, C.E.; KALMA, J.D.; BINNING, P.; WILLGOOSE, G.R.; VERTZONIS, M. Estimating evapotranspiration for a temperate salt marsh Newcastle, Australia,” *Hydrological Processes*, v. 15, p. 957-975, 2001. <http://dx.doi.org/10.1002/hyp.189>
- LI, S.-G.; EUGSTER, W.; ASANUMA, J; KOTANI, A.; DAVAA, G.; OYUNBAATAR, D.; SUGITA, M. Energy partitioning and its biophysical controls above a grazing steppe in central Mongólia. *Agricultural and Forest Meteorology*, v. 137, p. 89-106, 2006. <http://dx.doi.org/10.1016/j.agrformet.2006.03.010>
- PÔÇAS, I.; CUNHA, M.; PEREIRA, L.S.; ALLEN, R.G. Using remote sensing energy balance and evapotranspiration to characterize montane landscape vegetation with focus on grass and pasture lands. *International Journal of Applied Earth Observation and Geoinformation*, v.21, p. 159-172, 2013. <http://dx.doi.org/10.1016/j.jag.2012.08.017>
- TEIXEIRA, A.H. de C., BASTIAANSEN, W.G.M., AHMAD, M.D., BOS, M.G. Analysis of energy fluxes and vegetation-atmosphere parameters in irrigated and natural ecosystems of

semi-arid Brazil. *Journal of Hydrology*, v. 362, p. 110-127, 2008.
<http://dx.doi.org/10.1016/j.jhydrol.2008.08.011>

TEIXEIRA, A.H. de C.; BASTIAANSEN, W.G.M.; AHMAD, M-UD-D; BOS, M.G. Reviewing SEBAL input parameters for assessing evapotranspiration and water productivity for the Low-Middle São Francisco River basin, Brazil Part A: Calibration and validation. *Agricultural and Forest Meteorology*, v. 149, p. 462-476, 2009a.
<http://dx.doi.org/10.1016/j.agrformet.2008.09.016>

Teixeira, A.H. de C.; Bastiaanssen, W.G.M.; Ahmad, M.D.; Bos, M.G. Reviewing SEBAL input parameters for assessing evapotranspiration and water productivity for the Low-Middle São Francisco River basin, Brazil Part B: Application to the large scale. *Agricultural and Forest Meteorology*, v. 149, p. 477-490, 2009b.
<http://dx.doi.org/10.1016/j.agrformet.2008.09.014>

TEIXEIRA, A.H. de C.; HERNANDEZ, F.B.T.; LOPES, H.L.; SCHERER-WARREN, M.; BASSOI, L.H. A Comparative Study of Techniques for Modeling the Spatiotemporal Distribution of Heat and Moisture Fluxes in Different Agroecosystems in Brazil. In: G. PETROPOULOS. G. (Org.). *Remote Sensing of Energy Fluxes and Soil Moisture Content*. 1ed. Boca Raton, Florida: CRC Group, Taylor and Francis, 2014. p. 169-191

van DIJK, A.I.J.M.; BRUIJNZEEL, L.A.; SCHELLEKENS, J. Micrometeorology and water use of mixed crops in upland West Java, Indonesia. *Agricultural and Forest Meteorology*, v. 124, p. 31-49, 2004. <http://dx.doi.org/10.1016/j.agrformet.2004.01.006>

YUNUSA, I.A.M.; WALKER, R.R.; LU, P. Evapotranspiration components from energy balance, sapflow and microlysimetry techniques for an irrigated vineyard in inland Australia. *Agricultural and Forest Meteorology*, v. 127, p. 93-107, 2004.
<http://dx.doi.org/10.1016/j.agrformet.2004.07.001>

Table 1. Mean values of the energy balance components in the selected area of the Juazeiro municipality, Northeast Brazil, for each day of the year (DOY/Year), involving different thermo-hydrological conditions: (a) global solar radiation (R_G); (b) net radiation (R_n); latent heat flux (λE); sensible heat flux (H); soil heat flux (G); evaporative fraction (E_f).

DOY/Year	R_G (MJ m ⁻² d ⁻¹)	R_n (MJ m ⁻² d ⁻¹)	λE (MJ m ⁻² d ⁻¹)	H (MJ m ⁻² d ⁻¹)	G (MJ m ⁻² d ⁻¹)	E_f (-)
150/2013	21.0 ± 0.1	8.2 ± 0.2	9.2 ± 2.6	-1.4 ± 2.6	0.4 ± 0.1	1.2 ± 0.3
278/2013	26.2 ± 0.2	11.9 ± 0.3	7.5 ± 3.3	4.0 ± 3.3	0.4 ± 0.1	0.7 ± 0.3
153/2014	19.6 ± 0.5	8.8 ± 0.3	10.5 ± 2.3	-2.1 ± 2.3	0.4 ± 0.1	1.3 ± 0.3
265/2014	24.5 ± 0.2	10.0 ± 0.4	9.8 ± 2.7	-0.2 ± 2.8	0.4 ± 0.1	1.0 ± 0.3